

SUPPORTING INFORMATION

Hexa-nuclear molecular precursors as tools to design luminescent coordination polymers with lanthanides segregation.

Haiyun Yao^{a,b}, Guillaume Calvez^{a,*}, Carole Daiguebonne^{a,*}, Yan Suffren^a, Kevin Bernot^a and Olivier Guillou^a

^a Univ Rennes, INSA Rennes, CNRS UMR 6226 "Institut des Sciences Chimiques de Rennes", F-35708 Rennes, France.

^b Present address: School of Opto-electronic Engineering, Zaozhuang University, Zaozhuang 277160, China.

* To whom correspondence should be addressed.

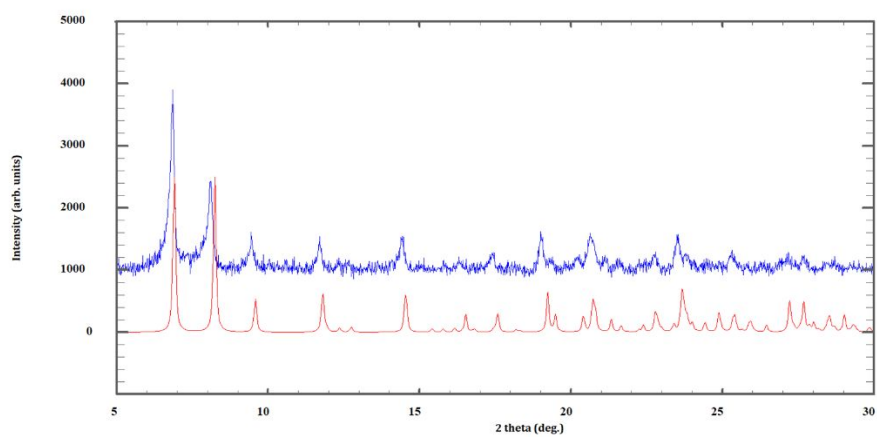


Figure S1. Experimental X-ray powder pattern of $[\text{Dy}_2(2\text{-bb})_6]_\infty$ (top) and simulated X-ray powder diagram of $[\text{Dy}_2(2\text{-bb})_6]_\infty$ from the crystal structure (bottom).

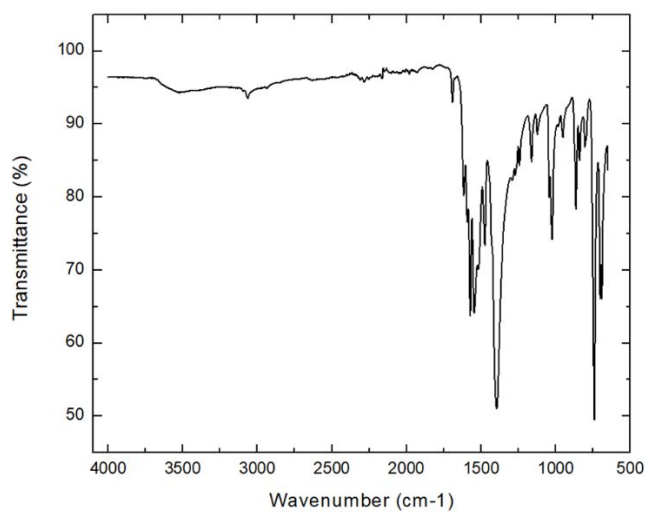


Figure S2. IR spectrum of $[\text{Dy}_2(2\text{-bb})_6]_\infty$.

Table S1. Shape calculations of the coordination polyhedrons of [Tb(4-fb)] _∞ , [Tb(4-cb)] _∞ , [Sm(4-bb)] _∞ , [Y(3-fb)] _∞ and [Tb(3-cb)] _∞ .													
[ML ₈]	OP-8	HPY-8	HBPY-8	CU-8	SAPR-8	TDD-8	JGBF-8	JETBPY-8	JBTPR-8	BTPR-8	JSD-8	TT-8	ETBPY-8
Dy1	28.648	22.165	11.445	10.690	4.964	3.577	9.284	22.608	3.938	3.720	2.958	11.415	21.447
OP-8 ≡ D8h-Octagon; HPY-8 ≡ C7v-Heptagonal pyramid; HBPY-8 ≡ D6h-Hexagonal bipyramid; CU-8 ≡ Oh-Cube; SAPR-8 ≡ 4d-Square antiprism; TDD-8 ≡ D2d-Triangular dodecahedron; JGBF-8 ≡ D2d-Johnson gyrobifastigium J26; JETBPY-8 ≡ D3h-Johnson elongated triangular bipyramid J14; JBTPR-8 ≡ C2v-Biaugmented trigonal prism J50; BTPR-8 ≡ C2v-Biaugmented trigonal prism; JSD-8 ≡ D2d-Snub diphenoid J84 ; TT-8 ≡ Td-Triakis tetrahedron; ETBPY-8 ≡ D3h-Elongated trigonal bipyramid.													
[ML ₇]	HP-7	HPY-7	PBPY-7	COC-7	CTPR-7	JPBPY-7	JETPY-7						
Dy2	29.905	23.824	1.119	7.501	5.933	3.806	22.701						
HP-7 ≡ D7h-Heptagon; HPY-7 ≡ C6v-Hexagonal pyramid; PBPY-7 ≡ D5h-Pentagonal bipyramid ; COC-7 ≡ C3v-Capped octahedron; CTPR-7 ≡ C2v-Capped trigonal prism; JPBPY-7 ≡ D5h-Johnson pentagonal bipyramid J13; JETPY-7 ≡ C3v-Johnson elongated triangular pyramid J7													

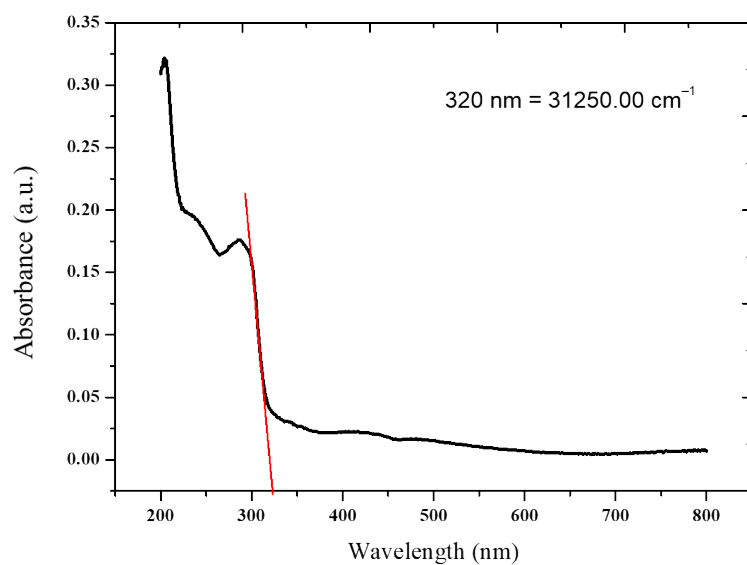


Figure S3. Room temperature solid-state absorption spectrum of $[\text{Y}_2(2\text{-bb})_6]_\infty$.

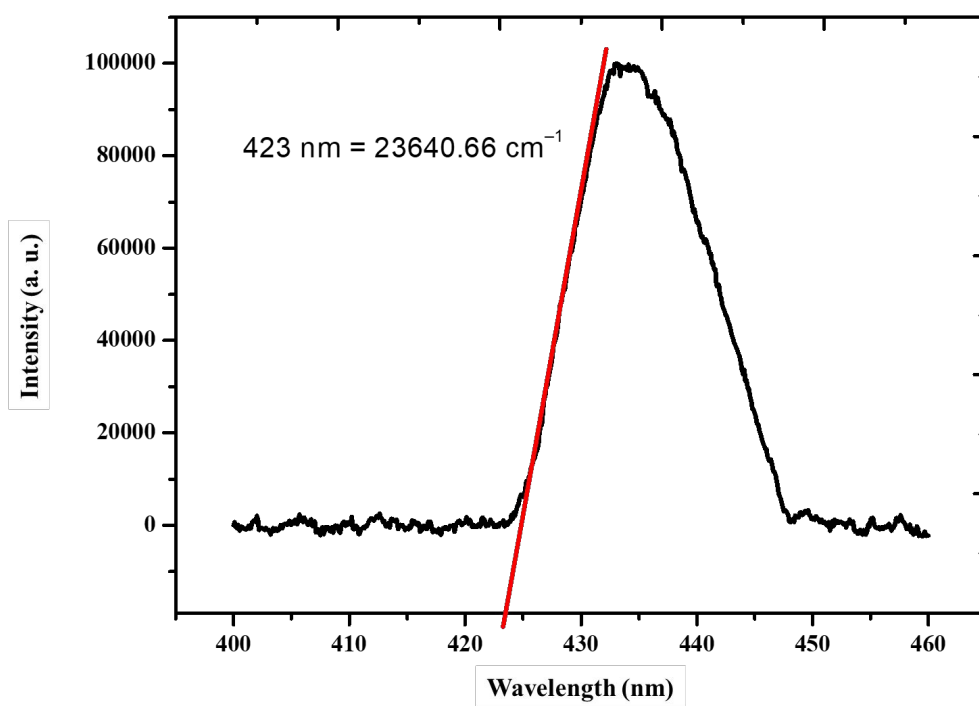


Figure S4. Solid-state emission spectrum of $[\text{Y}_2(2\text{-bb})_6]_\infty$ recorded at 77 K ($\lambda_{\text{exc}} = 300$ nm).

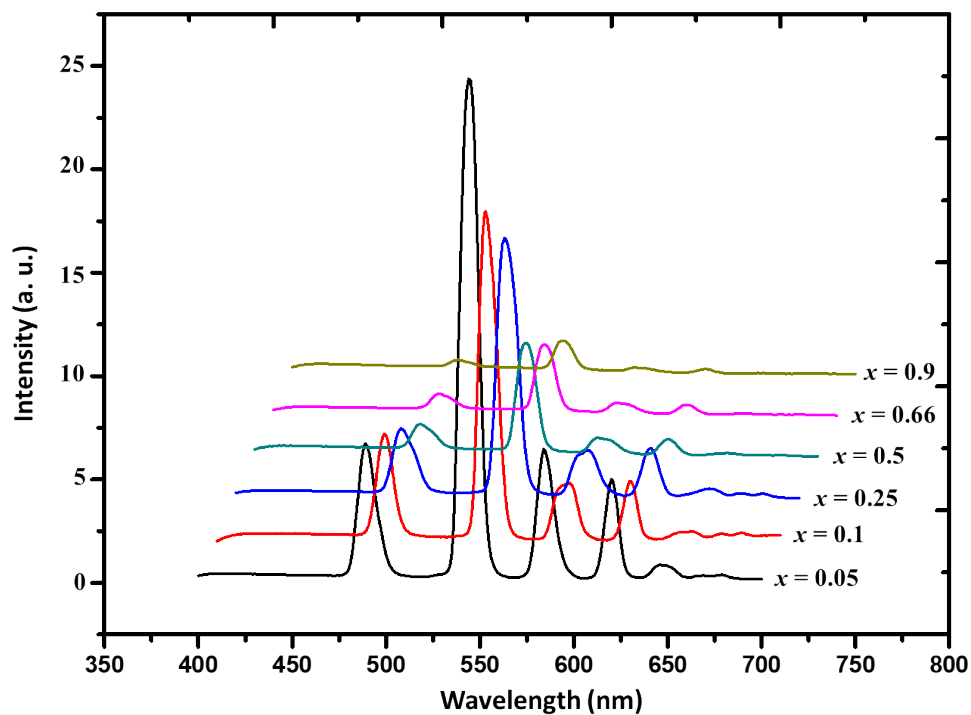


Figure S5. Room temperature solid-state emission spectra of $[\text{Y}_{2x}\text{Tb}_{2-2x}(\text{2-bb})_6]_{\infty}$ with $0.05 \leq x \leq 0.9$ ($\lambda_{\text{exc}} = 300 \text{ nm}$).

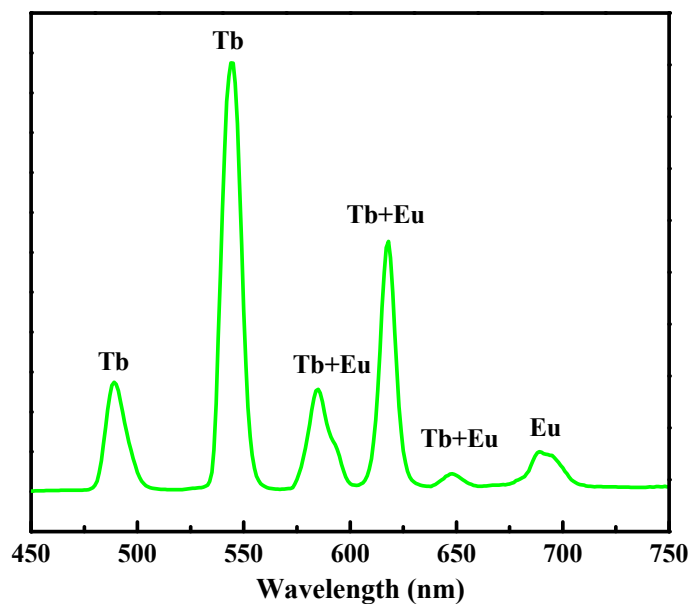


Figure S6. Room temperature solid-state emission spectrum of $\{[\text{Y}_2(\text{2-bb})_6]_{0.8}[\text{Tb}_2(\text{2-bb})_6]_{0.1}[\text{Eu}_2(\text{2-bb})_6]_{0.1}\}_{\infty}$ ($\lambda_{\text{exc}} = 300 \text{ nm}$).